2-Hydroxyglutarate magnetic resonance spectroscopy in adult brainstem glioma

Hirofumi Iwahashi, MD,[1] Hiroaki Nagashima, MD, PhD,[1] Kazuhiro Tanaka, MD, PhD,[1] Takiko Uno,[1] Mitsuru Hashiguchi, MD, PhD,[1] Masahiro Maeyama, MD, PhD,[1] Yuichiro Somiya,[2] Masato Komatsu, MD, PhD,[3] Takanori Hirose, MD, PhD,[4,5] Tomoo Itoh, MD, PhD,[3] Ryohei Sasaki, MD, PhD,[6] and Takashi Sasayama, MD, PhD[1]

Departments of [1]Neurosurgery, [3]Diagnostic Pathology, and [5]Pathology for Regional Communication, Kobe University Graduate School of Medicine, Kobe, Hyogo; [2]Division of Radiology, Kobe University Hospital, Kobe, Hyogo; [4]Department of Diagnostic Pathology, Hyogo Cancer Center, Akashi, Hyogo; and [6]Division of Radiation Oncology, Kobe University Graduate School of Medicine, Kobe, Hyogo, Japan

OBJECTIVE Adult brainstem gliomas (BSGs) are rare tumors of the CNS that are poorly understood. Upregulation of the oncometabolite 2-hydroxyglutarate (2HG) in the tumor indicates the mutation of isocitrate dehydrogenase (IDH), which can be detected by magnetic resonance spectroscopy (MRS). Although histological examination is required for the definitive diagnosis of BSG, 2HG-optimized MRS (2HG-MRS) may be useful, considering the difficult nature of brainstem lesion biopsy. The aim of this study was to evaluate the utility of 2HG-MRS for diagnosing IDH-mutant adult BSG.

METHODS Patients with a radiographically confirmed brainstem tumor underwent 3T MRS. A single voxel was set in the lesion with reference to the T2 or fluid-attenuated inversion recovery image and analyzed according to the 2HG-tailored MRS protocol (point-resolved spectroscopic sequence; echo time 35 msec). All patients underwent intraoperative navigation-guided or CT-guided stereotactic biopsy for histopathological diagnosis. The status of IDH and H3K27M mutations was confirmed by immunohistochemistry and direct DNA sequencing. In addition, the authors examined the relationship between patients' 2HG concentrations and survival time.

RESULTS Ten patients (7 men, 3 women; median age 33.5 years) underwent 2HG-MRS and biopsy. Four patients had an H3K27M mutation and 4 had an *IDH1* mutation (1 R132H canonical IDH mutation, 2 R132S and 1 R132G noncanonical IDH mutations). Two had neither H3K27M nor IDH mutations. The H3K27M and IDH mutations were mutually exclusive. Most tumors were located in the pons. There was no significant radiological difference between mutant H3K27M and IDH on a conventional MRI sequence. A 2HG concentration ≥ 1.8 mM on MRS demonstrated 100% (95% CI 28%–100%) sensitivity and 100% (95% CI 42%–100%) specificity for IDH-mutant BSG (p = 0.0048). The median overall survival was 10 months in IDH–wild-type BSG patients (n = 6) and could not be estimated in IDH-mutant BSG patients (n = 4) due to the small number of deaths (p = 0.008).

CONCLUSIONS 2HG-MRS demonstrated high sensitivity and specificity for the prediction of IDH-mutant BSG. In addition, 2HG-MRS may be useful for predicting the prognosis of adult BSG patients.

https://thejns.org/doi/abs/10.3171/2022.12.JNS221954

KEYWORDS adult brainstem glioma; magnetic resonance spectroscopy; IDH mutation; 2-hydroxyglutarate; 2HG; diagnosis; oncology; tumor

Aᴅᴜʟᴛ brainstem gliomas (BSGs) are rare and account for less than 2% of all gliomas in adults.[1,2] Adult BSGs are associated with a better patient prognosis than pediatric BSGs, but the average survival of patients with BSGs is still just 30 to 40 months.[3–7]

H3K27M mutation has been identified in high-grade gliomas arising from the thalamus, brainstem, and spinal cord as a diffuse midline glioma.[8] H3K27M mutation indicates lysine-to-methionine substitution at codon 27 in histone H3.3 (*H3F3A*) or H3.1 (*HIST1H3B/C*).[9,10] H3K27M
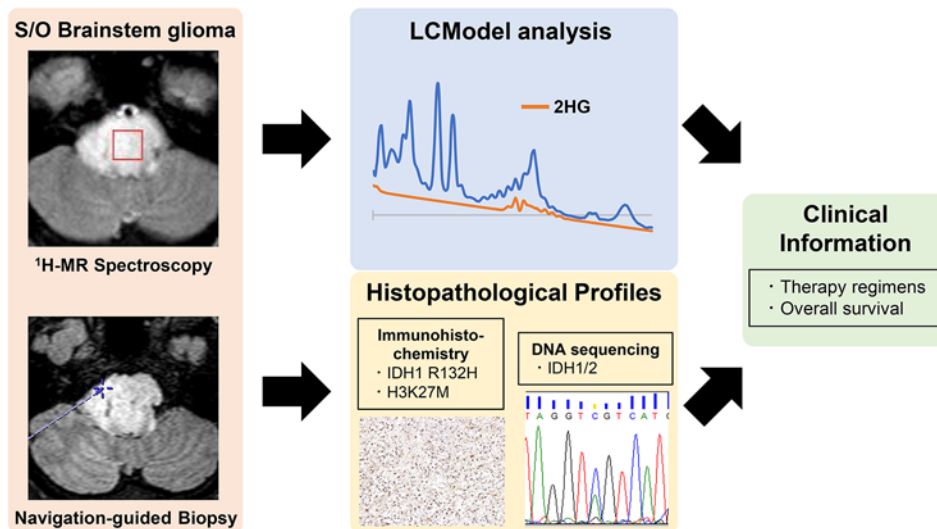
FIG. 1. Integrative analysis of 2HG detection in 3T MRS and histopathological/molecular and clinical information. The designation of tissue targets from in vivo MRS was analyzed using an LCModel. Stereotactic navigation (Brainlab AG)–guided sampling was performed at the exact targets indicated by MRS. The *red box* indicates the MRS VOI. Spectra were obtained with PRESS at a short echo time (35 msec). IDH and H3K27M status was assessed via immunohistochemical staining and direct sequencing. S/O = suspect of. Figure is available in color online only.

mutation is most common in young children but may also be seen in adults.[10] In particular, adult BSG with H3K27M mutation is known for its poor prognosis with a median survival of 10–20 months.[11–13]

In contrast, adult BSG with a mutation in the isocitrate dehydrogenase (IDH) genes *IDH1* and *IDH2* has a median survival of 43.8–141 months.[14–17] IDH converts isocitrate to α-ketoglutarate (αKG), and mutant IDH further converts αKG to D-2-hydroxyglutarate (2HG).[18] Therefore, 2HG can be used as a biomarker of IDH mutation status. Moreover, H3K27M and IDH mutations are mutually exclusive.[16] Therefore, the diagnosis of H3K27M and IDH status has major significance for treatment strategy planning and predicting BSG prognosis.

BSGs have often been diagnosed based on MRI findings or histopathological examination. Although MRI can be useful for diagnosis, the prediction of molecular status can be difficult.[19] While histological examination has been required for definitive diagnosis since the 2016 World Health Organization (WHO) Classification of Tumors of the Central Nervous System was published, because of the difficulty of obtaining tissue from the brainstem, a noninvasive tool is needed to determine the molecular features of BSGs and predict their clinical course. Recent studies have reported that magnetic resonance spectroscopy (MRS) can noninvasively provide the tissue 2HG concentration for supratentorial gliomas.[20–23] Here, we sought to determine 2HG in BSGs using MRS and found a high concentration of 2HG in IDH-mutant BSG. We examined the utility of 2HG-optimized MRS (2HG-MRS) for predicting the molecular profile and prognosis of adult BSGs.

Methods
Patient and Clinical Data

This study was approved by the ethics review boards of our institutions. Informed consent was obtained from each patient.

Among glioma patients diagnosed and treated at the Department of Neurosurgery, Kobe University Hospital, from July 2005 to May 2022, 10 patients were included in this study. Study inclusion criteria were as follows: 1) newly diagnosed gliomas localized to the brainstem (midbrain, pons, and medulla oblongata); 2) MRI and MRS performed preoperatively; 3) biopsy using an intraoperative navigation system (Brainlab AG) or Komai's CT-guided stereotactic apparatus (Mizuho) performed before initial treatment; and 4) postoperative treatment including radiation and/or chemotherapy received.

We retrospectively reviewed the medical records of patients and collected clinical data including age at admission, sex, lesion location, MRI appearance, 2HG concentration and other parameters of MRS, histopathological diagnosis, IDH/H3K27M mutation, O^6-methylguanine-DNA methyltransferase (*MGMT*) methylation, Ki-67 labeling index, treatment information, and overall survival (OS). The 2HG concentration at the brainstem lesion obtained by MRS was compared with the histopathological findings (Fig. 1).

As a comparison group, 3 patients with suspected BSG were included. They had brainstem lesions and underwent MRI and MRS at admission but not biopsy.

MRI and MRS Protocols

The MRS signal was acquired with a 3T MRI/^{1}H-MRS scanner (Achieva, Philips Medical Systems). An 8-channel head MRI coil was used for signal reception, and the quadrature body MRI coil was used for transmission of the radiofrequency pulses. After routine preoperative MRI, fluid-attenuated inversion recovery (FLAIR) and T2*-weighted images were obtained to localize the corre-

sponding target. Single-voxel localized MR spectra were acquired using a double-echo point-resolved spectroscopic sequence (PRESS) with chemical-shift selective water suppression. The MRS acquisition parameters were as follows: volume of interest (VOI) 1.5 × 1.5 × 1.5 cm^3, TR/TE 2000/35 msec, average number of acquisitions 128, and 1024 complex points for the spectral data. VOIs were localized to representative areas of the solid tumor. Regions of necrosis, hemorrhage, or peripheral edema were excluded from the corresponding region. The unsuppressed water signal was obtained using the abovementioned parameters. The full width at half maximum (FWHM) and signal-to-noise ratio (SNR) were assessed in the MR spectra. MRS data were quantified with LCModel version 6.3-1R (Stephen Provencher) using a basis set, developed by using MR experiment simulation software (GAMMA; Department of Radiology, Duke University Medical Center, Durham, North Carolina), and were calibrated with an MRS phantom. Metabolites were quantified with Cramer-Rao lower bounds (CRLBs). The CRLB values were calculated from the residual error and the Fisher matrix of the partial derivatives of the concentrations.[24] These CRLB values reflect the variance of the spectra fitting estimate but not its accuracy, and they indicate how close repeated measurements will be to the present measurement under similar experimental conditions.

Histopathological Diagnosis

Formalin-fixed paraffin-embedded tissue was used for histopathological diagnosis and molecular studies, and fresh-frozen tissue was used for DNA sequencing for IDH status and *MGMT* promoter methylation status. Histopathological diagnosis and WHO grading of tissues were performed by a board-certified neuropathologist (T.H.) following the 2021 WHO Classification of Tumors of the Central Nervous System. Molecular status was analyzed using immunohistochemistry (IHC) for *IDH1* R132H (clone H09, 1:15 dilution, mouse monoclonal antibody; Dianova) and Ki-67 (clone MIB-1, 1:5 dilution, mouse monoclonal antibody; DAKO Agilent Technologies). IHC for H3K27M mutation was performed as previously described[9] (1:1000 dilution, rabbit polyclonal antibody; Millipore). IDH mutation status was analyzed by IHC for *IDH1* R132H and by direct DNA sequencing of *IDH1* and *IDH2*.

Genomic DNA was isolated from frozen tissue using the DNeasy FFPE kit (Qiagen) according to the manufacturer's instructions. To identify the IDH mutations, forward and reverse primers were designed to amplify exon 4 (codon R132) of the *IDH1* gene and exon 4 (codon R172) of the *IDH2* gene. Polymerase chain reaction (PCR) was performed using the following primers for *IDH1* R132: sense, 5′-TGAGAAGAGG GTTGAGGAGT TCAAGT-3′; antisense, 5′-AATGTGTTGA GATG-GACGCC TATTTGT-3′; and for *IDH2* R172: sense, 5′- CCACTATTAT CTCTGTCCTC-3′; antisense, 5′-GCTAGGCGAG GAGCTCCAGT-3′. The primers and a MinElute PCR Purification Kit (Qiagen) were used to purify the PCR products. Then, the DNA sequence was analyzed, and the presence or absence of mutations was assessed using an Applied Biosystems DNA sequencer

in the hotspot codons R132 in *IDH1* and R140 and R172 in *IDH2*.

MGMT promoter methylation status was analyzed using a quantitative methylation-specific PCR assay as previously described.[25]

Statistical Analysis

Statistical analyses and graph construction were performed using Prism version 9 (GraphPad Software Inc.). Comparisons of OS were assessed graphically and using a log-rank test. We applied a 2HG cutoff value of 1.8 mM to discriminate mutant IDH from wild-type IDH according to the previous report.[23] The sensitivity, specificity, positive predictive value, and negative predictive value were calculated and tested using Fisher's exact test.

Results
Patient Characteristics

Ten patients were included. The patient characteristics are summarized in Table 1. There were 3 female patients (30%), and the median age at admission was 33.5 years (range 21–83 years). The predominant tumor location was the pons in all patients; 5 of the 10 tumors extended to the medulla oblongata. Contrast enhancement on MRI was seen in 3 cases, and tumor calcification was not observed in any patient. All 10 patients underwent MRS at admission. In all patients, the SNR was > 4 and the FWHM was < 0.08. Five of the 10 patients (cases 1, 2, 5, 6, and 9) received chemotherapy with temozolomide and radiotherapy (54–60 Gy/27–30 fractions). Five patients (cases 3, 4, 7, 8, and 10) received radiotherapy only. Illustrative cases (cases 1 and 9) are shown in Fig. 2. The MR spectra of all cases are shown in Supplementary Fig. S1.

2HG-MRS Study and Histopathology

Ten patients underwent tumor biopsy following MRS. Stereotactic and/or navigation-guided biopsy was performed in 5 patients, and navigation-guided open biopsy was performed in 5 patients. No patients developed surgery-related complications. On IHC, 4 patients were positive for H3K27M (cases 2, 5, 6, and 9) and were therefore diagnosed with diffuse midline glioma (WHO grade 4). On IHC for canonical *IDH1* R132H, only 1 patient (case 7) was positive. However, DNA sequence analysis of *IDH1* and *IDH2* revealed an *IDH1* R132G mutation in case 1 and an *IDH1* R132S mutation in cases 3 and 8; both are noncanonical IDH mutations. *IDH2* mutation was not detected in any patient. In these patients, preoperative MRS showed a high 2HG concentration. In contrast, cases 2, 4–6, 9, and 10 had wild-type IDH, and their preoperative MRS showed no or low concentrations of 2HG (< 1.8 mM) (Fig. 3A). Cases 4 and 10 had neither IDH mutation nor H3K27M mutation. A 2HG concentration ≥ 1.8 mM demonstrated 100% (95% CI 28%–100%) sensitivity and 100% (95% CI 42%–100%) specificity for IDH-mutant glioma, and this cutoff value was statistically significant (p = 0.0048, Fisher's exact test). The median Ki-67 labeling index was 7.5 (range 1–60). *MGMT* methylation was detected in 3 patients (cases 7–9).

TABLE 1. Patient characteristics of adult BSG with biopsy

Case No.	Age (yrs)	Sex	MRI Location	MRI CE	MRS 2HG (mM)	MRS SNR	MRS FWHM	Operation	Pathological Diagnosis	IDH Status	H3K27M Mutation	MGMT Methylation	Ki-67 Labeling Index (%)	Treatment	OS (mos)	Status
1	27	M	Pons & cerebellar peduncle	−	4.38	8	0.046	Komai stereotactic biopsy	Astrocytoma, IDH-mutant, grade 2	IDH1 R132G mutation	No	UM	3	RT+TMZ	63	Dead
2	65	M	Pons	+	0.965	7	0.038	Komai stereotactic biopsy	Diffuse midline glioma	Wild type	Yes	UM	5	RT+TMZ	3	Dead
3	24	M	Pons & medulla	−	4.897	6	0.061	Navigation-guided open biopsy	Astrocytoma, IDH-mutant, grade 2	IDH1 R132S mutation	No	UM	3	RT	64	Alive
4	21	M	Pons	−	1.311	6	0.076	Komai stereotactic biopsy	Glioblastoma, IDH-wildtype	Wild type	No	UM	5	RT	39	Dead
5	53	M	Pons & medulla	−	0	10	0.046	Navigation-guided open biopsy	Diffuse midline glioma	Wild type	Yes	UM	10	RT+TMZ	10	Dead
6	34	M	Pons & medulla	+	1.711	6	0.076	Navigation-guided open biopsy	Diffuse midline glioma	Wild type	Yes	UM	10	RT+TMZ	25	Dead
7	33	F	Pons & medulla	−	4.788	7	0.061	Navigation-guided open biopsy	Astrocytoma, IDH-mutant, grade 2	IDH1 R132H mutation	No	M	<1	RT	26	Alive
8	38	M	Pons & medulla	−	2.02	10	0.054	Navigation-guided open biopsy	Astrocytoma, IDH-mutant, grade 2	IDH1 R132S mutation	No	M	10	RT	201	Alive
9	25	F	Pons	−	0	7	0.069	Navigation-guided needle biopsy	Diffuse midline glioma	Wild type	Yes	M	60	RT+TMZ	6	Alive
10	83	F	Pons & cerebellar peduncle	+	0	5	0.092	Navigation-guided needle biopsy	High-grade glioma, NOS	Wild type	No	UM	35	RT	4	Dead

CE = contrast enhancement; M = methylated; NOS = not otherwise specified; RT = radiation therapy; TMZ = temozolomide; UM = unmethylated; + = present; − = absent.
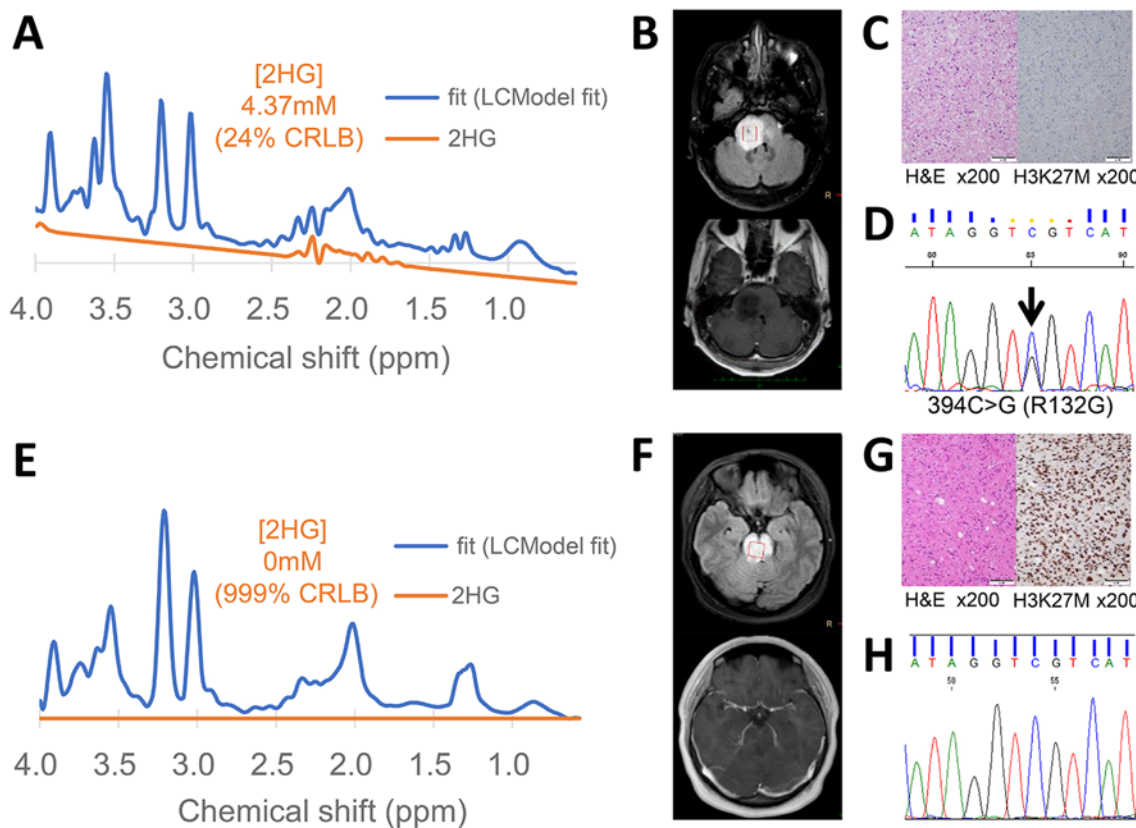
FIG. 2. Representative cases of IDH-mutant (case 1) and IDH–wild-type (case 9) BSGs. Case 1. **A and B:** Preoperative MR spectra (A) and axial T2-FLAIR (B, *upper*) and contrast-enhanced T1-weighted (B, *lower*) images obtained in a 27-year-old man with an IDH-mutated BSG. The T2-FLAIR image shows a diffuse high-signal-intensity lesion in the pons. The *red box* indicates the MRS VOI. The Gd-enhanced T1-weighted image shows an hypointense lesion without contrast enhancement. The 2HG concentration was estimated to be 4.37 mM (± 24% CRLB). **C:** The hematoxylin and eosin (H&E)–stained section (*left*) shows diffusely infiltrating tumor cells with mild nuclear atypia. No mitoses, necrosis, or microvascular proliferation are seen. Immunohistochemical staining for H3K27M mutation (*right*) is negative. **D:** Direct DNA sequencing identified the *IDH1* R132G mutation (394C>G, *black arrow*). Case 9. **E and F:** Preoperative MR spectra (E) and axial T2-FLAIR (F, *upper*) and Gd-enhanced T1-weighted (F, *lower*) MR images obtained in a 25-year-old woman with an H3K27M-mutant BSG. The T2-FLAIR image shows a diffuse high-signal-intensity lesion in the pons. The *red box* indicates the MRS VOI. The Gd-enhanced T1-weighted image shows an isointense lesion without contrast enhancement. MRS shows no 2HG peak. **G:** The H&E-stained section (*left*) shows diffuse proliferation of anaplastic tumor cells. Necrosis and microvascular proliferation are not present. Immunohistochemical staining for H3K27M mutation (*right*) shows that most tumor cells were positive. **H:** Direct DNA sequencing identified no *IDH1/2* mutation. Figure is available in color online only.

OS Study

The duration of follow-up ranged from 1 to 198 months. The median OS was 10 months in IDH–wild-type BSG patients (n = 6) but could not be estimated for IDH-mutant BSG patients (n = 4) because of the small number of deaths. The Kaplan-Meier curve revealed a better OS in patients with IDH mutation (p = 0.008) (Fig. 3B). Patients with contrast enhancement on MRI (n = 3) had worse survival, with a median OS of 15 months compared with a median OS of 65 months in patients without contrast enhancement (n = 7) (p = 0.034). There was no statistically significant difference in OS between patients with *MGMT* methylation and those without (p = 0.121). There were no significant differences in the levels of MRS metabolites such as total choline, total *N*-acetylaspartic acid (NAA), glutamate, glutamine, and creatine between mutant and wild-type IDH.

Among the 3 patients without biopsy, one with increased 2HG on MRS had better survival (111 months). The other 2 patients with contrast enhancement on MRI but no increase in 2HG had shorter survival (4 and 30 months).

Discussion

Here, we report the utility of noninvasive 2HG-MRS for predicting the molecular profile/patient survival in 10 radiographically identified brainstem tumors. The molecular biology of adult BSGs is not well understood because of its low prevalence and difficult biopsy. For supratentorial glioma, 2HG-MRS is widely available as a noninvasive diagnostic tool for IDH mutation. In contrast, for BSG, there are no reports highlighting 2HG-MRS with biopsy validation of the molecular information. Recent reports have shown that the commonly mutated genes in
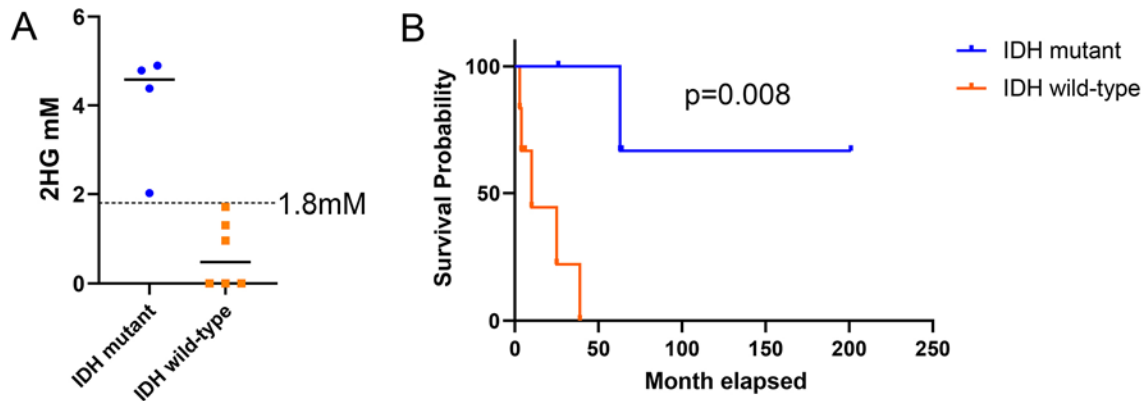
FIG. 3. A high 2HG concentration predicts IDH mutation and better prognosis for patients with BSGs. **A:** The 2HG concentration on MRS in 10 BSG patients. The *solid line* shows the median. The cutoff value of 1.8 mM (*dashed line*) demonstrates 100% sensitivity and 100% specificity (p = 0.0048, Fisher's exact test). **B:** Kaplan-Meier plot of the OS of IDH-mutant and IDH–wild-type BSGs showing that IDH-mutant BSG was associated with longer patient survival (p = 0.008, log-rank test). The median OS was 10 months for patients with IDH–wild-type BSG (n = 6) and could not be estimated in IDH-mutant BSG (n = 4) because of the small number of deaths. Figure is available in color online only.

adult BSGs are H3K27M and *IDH1*; the two mutations are mutually exclusive.[16,26] A recent study of 17 diffuse adult BSGs suggested that their characteristics differ from those of supratentorial glioma in adults.[27] Another recent study reported histone *H3F3A* K27M alterations in 15 of 28 samples (53.6%) of adult midline BSGs.[13] Furthermore, the presence of the *H3F3A* K27M mutation was associated with a worse OS.[13] In the present study, the H3K27M mutation was identified in 4 of the 10 tumors (40%).

In contrast, the presence of IDH mutation in adult BSGs is reported to have better prognosis.[14,15] Wang et al. detected an *IDH1* mutation in 26.5% (13 of 49 cases) of BSGs.[14] Wild-type IDH converts isocitrate to αKG, whereas mutant IDH further converts αKG to 2HG.[18] Although there are several types of IDH mutations, *IDH1* R132H is the most frequent subtype among supratentorial gliomas. Interestingly, IDH variants are rarely found in supratentorial astrocytomas, while *IDH1* R132C and R132G are more frequently detected in infratentorial astrocytomas.[28] A previous report found that only 3 of 43 patients had an *IDH1* R132H mutation in BSG.[27] Another report showed that 1 of 17 patients had an R132H mutation and that 2 of 17 patients had *IDH1* R132C and R132G mutations, suggesting that BSGs may have rare IDH mutations.[11] Similarly, in the DNA sequence analysis performed in the present study, the patient in case 1 had an *IDH1* R132G mutation and patients in cases 3 and 8 had an *IDH1* R132S mutation; both mutations are considered rare IDH mutations. IHC for *IDH1* R132H, even with an antibody commonly used in IHC, may be insufficient to diagnose adult BSGs. Therefore, MRS might be more useful than IHC in BSG because it can directly detect 2HG produced by mutant IDH.[29]

It has been difficult to speculate about the histopathology of gliomas based on radiological appearance because tumors with similar MRI findings can have differing molecular pathologies. Approximately 60% of BSGs are located in the center of the pons, but they can also arise from the midbrain and medulla oblongata.[2] The MRI features of adult BSGs are characterized as T1-hypointense and T2-hyperintense masses, with approximately 40% contrast enhancement.[30] Meyronet et al. showed that 50% of H3K27M-mutant diffuse midline gliomas demonstrated contrast enhancement.[10] Aboian et al. reported no significant differences in radiographic features between tumors with and without H3K27M mutation,[19] while Wang et al. reported that H3K27M mutation and contrast enhancement on MRI imparted a worse prognosis.[14] In the present study, 2 of the 4 BSGs (cases 2 and 6) with the H3K27M mutation had contrast enhancement, but cases 5 and 9 had no enhancement. It is difficult to make a histopathological diagnosis and prognosis based on the contrast findings on MRI alone. Significant effort has been devoted to the development of MRI-based radiogenomics for IDH status prediction. Manikis et al. reported the use of dynamic susceptibility contrast MRI (DSC-MRI) in gliomas for IDH status subtyping.[31] In addition, Han et al. identified T2-FLAIR mismatch sign as a noninvasive imaging biomarker for the selection of patients with IDH-mutant lower-grade gliomas.[32]

Conventional MRS, with an increase in the lactate peak and in the choline/NAA ratio due to a decrease in the NAA signal, can be useful for the diagnosis of BSGs,[33] but there is currently no effective tool based on molecular findings. Previous studies have demonstrated that 2HG on MRS may be a biomarker for IDH mutation status for supratentorial glioma,[20,23] but the usefulness of MRS for BSG was unknown. Thus, we focused on the detection of 2HG using MRS, and we evaluated the diagnostic value of MRS in adult BSG.

Single-voxel ^{1}H-MRS for brainstem lesions might be challenging because bone artifacts and small-sized anatomical structures cause inhomogeneity of the main magnetic field and complicate shimming, whereas BSG with diffuse swelling might be a suitable target for MRS because of a lower influence of the cerebrospinal fluid in VOI establishment. In addition, regions of necrosis, hemorrhage, or calcification, which lead to false-positive and false-negative results, were relatively rare in our cohort.

Previous reports also noted that BSGs had less calcification and necrosis.[34,35] Therefore, 2HG-MRS of BSGs achieved high detection accuracy (100% sensitivity and specificity) for IDH mutation. Our results indicated that single-voxel ^{1}H-MRS for adult BSGs using conventional methods was clinically acceptable.

In this study, we identified IDH mutation using only the 2HG concentration on MRS. Other studies have suggested that the 2HG/(lipid + lactate) ratio[36] or a combination of 2HG and glutamate[23] can provide higher diagnostic accuracy than 2HG alone. We evaluated the clinical MRS data, but there were no significant differences in MRS metabolite levels, including total choline, total NAA, glutamate, glutamine, and creatine, between mutant and wild-type IDH.

It had been controversial whether biopsy should be performed in cases of suspected BSG due to the difficulty of obtaining tissue from the brainstem. Since the 2016 WHO Classification of Tumors of the Central Nervous System was published, molecular information has been essential for diagnosis. Recently, Hersh et al. reported that brainstem biopsy was safe and efficacious in children and young adults.[37] Indeed, we performed biopsies on 10 BSG patients without complication. Nevertheless, there are cases in which enough tissue cannot be obtained by biopsy or in which the biopsy itself is difficult. Direct DNA sequencing can detect both canonical and noncanonical IDH mutations. However, it is not available in all laboratories and cannot be performed with small amounts of tissue. In contrast, MRS can be performed noninvasively and repeatedly. We expect 2HG-MRS to be a complementary tool used in the differential diagnosis of a brainstem lesion and suspected noncanonical IDH mutation, prognosis estimation, and treatment monitoring.

This work has several limitations. First, the study was based on only 10 patients. In general, patients with IDH mutation have better prognosis, but this relationship is unclear for BSG. Wang et al. reported that IDH-mutant BSGs were associated with better OS compared with wild-type IDH in their review of 96 BSG patients.[14] Although adult BSG has a low prevalence, a larger number of patients should be included to validate our findings. Second, the VOI was manually set according to the MR image, so bias may occur depending on the examiner and MRI device. In addition, we examined only 3T short-echo-time MRS. In a conventional 3T MRS study,[20,23] this application was widely available for clinical use on all scanners without spectral editing. However, there was a high incidence of false-positive and false-negative results. Recently, customized MRS techniques using spectral editing and asymmetrical long-echo-time MRS (echo time 97 msec) have been reported to more reliably detect 2HG.[38] Moreover, the usefulness of 7–9.4T 2HG-MRS has been reported.[39–41] These techniques should thus be applied to BSG. Third, in the present study, some IDH–wild-type BSGs had a slightly elevated 2HG concentration. The reported cutoff value for 2HG concentration varies from 0.897 to 2,[42] and thus further study is needed to determine the optimal cutoff value. Finally, metabolome analysis should be performed to confirm 2HG levels in tissue, but the amount of tissue that can be safely collected by brainstem lesion biopsy is limited.

Conclusions

We described 10 cases of adult BSG in which 2HG was a predictive biomarker for IDH mutation and prognosis. The noninvasive detection of 2HG by MRS might be useful in the clinical management of patients with adult BSG.

Acknowledgments

References

1. Reyes-Botero G, Mokhtari K, Martin-Duverneuil N, Delattre JY, Laigle-Donadey F. Adult brainstem gliomas. *Oncologist.* 2012;17(3):388-397.
2. Grimm SA, Chamberlain MC. Brainstem glioma: a review. *Curr Neurol Neurosci Rep.* 2013;13(5):346.
3. Guillamo JS, Monjour A, Taillandier L, et al. Brainstem gliomas in adults: prognostic factors and classification. *Brain.* 2001;124(Pt 12):2528-2539.
4. Babu R, Kranz PG, Agarwal V, et al. Malignant brainstem gliomas in adults: clinicopathological characteristics and prognostic factors. *J Neurooncol.* 2014;119(1):177-185.
5. Kesari S, Kim RS, Markos V, Drappatz J, Wen PY, Pruitt AA. Prognostic factors in adult brainstem gliomas: a multicenter, retrospective analysis of 101 cases. *J Neurooncol.* 2008;88(2):175-183.
6. Rineer J, Schreiber D, Choi K, Rotman M. Characterization and outcomes of infratentorial malignant glioma: a population-based study using the Surveillance Epidemiology and End-Results database. *Radiother Oncol.* 2010;95(3):321-326.
7. Hundsberger T, Tonder M, Hottinger A, et al. Clinical management and outcome of histologically verified adult brainstem gliomas in Switzerland: a retrospective analysis of 21 patients. *J Neurooncol.* 2014;118(2):321-328.
8. López G, Oberheim Bush NA, Berger MS, Perry A, Solomon DA. Diffuse non-midline glioma with *H3F3A* K27M mutation: a prognostic and treatment dilemma. *Acta Neuropathol Commun.* 2017;5(1):38.
9. Castel D, Philippe C, Calmon R, et al. Histone *H3F3A* and *HIST1H3B* K27M mutations define two subgroups of diffuse intrinsic pontine gliomas with different prognosis and phenotypes. *Acta Neuropathol.* 2015;130(6):815-827.
10. Meyronet D, Esteban-Mader M, Bonnet C, et al. Characteristics of H3 K27M-mutant gliomas in adults. *Neuro Oncol.* 2017;19(8):1127-1134.
11. Reuss DE, Kratz A, Sahm F, et al. Adult *IDH* wild type astrocytomas biologically and clinically resolve into other tumor entities. *Acta Neuropathol.* 2015;130(3):407-417.
12. Aihara K, Mukasa A, Gotoh K, et al. *H3F3A* K27M mutations in thalamic gliomas from young adult patients. *Neuro Oncol.* 2014;16(1):140-146.
13. Feng J, Hao S, Pan C, et al. The H3.3 K27M mutation results in a poorer prognosis in brainstem gliomas than thalamic gliomas in adults. *Hum Pathol.* 2015;46(11):1626-1632.
14. Wang Y, Pan C, Xie M, et al. Adult diffuse intrinsic pontine glioma: clinical, radiological, pathological, molecular features, and treatments of 96 patients. *J Neurosurg.* 2022;137(6):1628-1638.
15. Chen LH, Pan C, Diplas BH, et al. The integrated genomic and epigenomic landscape of brainstem glioma. *Nat Commun.* 2020;11(1):3077.
16. Sturm D, Witt H, Hovestadt V, et al. Hotspot mutations in *H3F3A* and *IDH1* define distinct epigenetic and biological subgroups of glioblastoma. *Cancer Cell.* 2012;22(4):425-437.

17. Poetsch L, Bronnimann C, Loiseau H, et al. Characteristics of *IDH*-mutant gliomas with non-canonical *IDH* mutation. *J Neurooncol*. 2021;151(2):279-286.

18. Dang L, Yen K, Attar EC. IDH mutations in cancer and progress toward development of targeted therapeutics. *Ann Oncol*. 2016;27(4):599-608.

19. Aboian MS, Solomon DA, Felton E, et al. Imaging characteristics of pediatric diffuse midline gliomas with histone H3 K27M mutation. *AJNR Am J Neuroradiol*. 2017;38(4):795-800.

20. Tietze A, Choi C, Mickey B, et al. Noninvasive assessment of isocitrate dehydrogenase mutation status in cerebral gliomas by magnetic resonance spectroscopy in a clinical setting. *J Neurosurg*. 2018;128(2):391-398.

21. Choi C, Raisanen JM, Ganji SK, et al. Prospective longitudinal analysis of 2-hydroxyglutarate magnetic resonance spectroscopy identifies broad clinical utility for the management of patients with *IDH*-mutant glioma. *J Clin Oncol*. 2016; 34(33):4030-4039.

22. Pope WB, Prins RM, Albert Thomas M, et al. Non-invasive detection of 2-hydroxyglutarate and other metabolites in *IDH1* mutant glioma patients using magnetic resonance spectroscopy. *J Neurooncol*. 2012;107(1):197-205.

23. Nagashima H, Tanaka K, Sasayama T, et al. Diagnostic value of glutamate with 2-hydroxyglutarate in magnetic resonance spectroscopy for *IDH1* mutant glioma. *Neuro Oncol*. 2016; 18(11):1559-1568.

24. Graveron-Demilly D. Quantification in magnetic resonance spectroscopy based on semi-parametric approaches. *MAGMA*. 2014;27(2):113-130.

25. Vlassenbroeck I, Califice S, Diserens AC, et al. Validation of real-time methylation-specific PCR to determine O^6-methylguanine-DNA methyltransferase gene promoter methylation in glioma. *J Mol Diagn*. 2008;10(4):332-337.

26. Eisele SC, Reardon DA. Adult brainstem gliomas. *Cancer*. 2016;122(18):2799-2809.

27. Salmaggi A, Fariselli L, Milanesi I, et al. Natural history and management of brainstem gliomas in adults. A retrospective Italian study. *J Neurol*. 2008;255(2):171-177.

28. Banan R, Stichel D, Bleck A, et al. Infratentorial IDH-mutant astrocytoma is a distinct subtype. *Acta Neuropathol*. 2020; 140(4):569-581.

29. Choi C, Ganji SK, DeBerardinis RJ, et al. 2-Hydroxyglutarate detection by magnetic resonance spectroscopy in IDH-mutated patients with gliomas. *Nat Med*. 2012;18(4):624-629.

30. Dellaretti M, Touzet G, Reyns N, et al. Correlation between magnetic resonance imaging findings and histological diagnosis of intrinsic brainstem lesions in adults. *Neuro Oncol*. 2012;14(3):381-385.

31. Manikis GC, Ioannidis GS, Siakallis L, et al. Multicenter DSC–MRI-based radiomics predict IDH mutation in gliomas. *Cancers (Basel)*. 2021;13(16):3965.

32. Han Z, Chen Q, Zhang L, et al. Radiogenomic association between the T2-FLAIR mismatch sign and IDH mutation status in adult patients with lower-grade gliomas: an updated systematic review and meta-analysis. *Eur Radiol*. 2022;32(8): 5339-5352.

33. Porto L, Hattingen E, Pilatus U, et al. Proton magnetic resonance spectroscopy in childhood brainstem lesions. *Childs Nerv Syst*. 2007;23(3):305-314.

34. Ueoka DI, Nogueira J, Campos JC, Maranhão Filho P, Ferman S, Lima MA. Brainstem gliomas—retrospective analysis of 86 patients. *J Neurol Sci*. 2009;281(1-2):20-23.

35. Lee BCP, Kneeland JB, Walker RW, Posner JB, Cahill PT, Deck MD. MR imaging of brainstem tumors. *AJNR Am J Neuroradiol*. 1985;6(2):159-163.

36. Suh CH, Kim HS, Park JE, et al. Comparative value of 2-hydroxyglutarate–to–lipid and lactate ratio versus 2-hydroxyglutarate concentration on MR spectroscopic images for predicting isocitrate dehydrogenase mutation status in gliomas. *Radiol Imaging Cancer*. 2020;2(4):e190083.

37. Hersh DS, Kumar R, Moore KA, et al. Safety and efficacy of brainstem biopsy in children and young adults. *J Neurosurg Pediatr*. 2020;26(5):552-562.

38. Choi C, Ganji S, Hulsey K, et al. A comparative study of short- and long-TE ¹H MRS at 3 T for *in vivo* detection of 2-hydroxyglutarate in brain tumors. *NMR Biomed*. 2013; 26(10):1242-1250.

39. Ganji SK, An Z, Tiwari V, et al. *In vivo* detection of 2-hydroxyglutarate in brain tumors by optimized point-resolved spectroscopy (PRESS) at 7T. *Magn Reson Med*. 2017;77(3): 936-944.

40. Provencher SW. Automatic quantitation of localized *in vivo* ¹H spectra with LCModel. *NMR Biomed*. 2001;14(4):260-264.

41. Verma G, Mohan S, Nasrallah MP, et al. Non-invasive detection of 2-hydroxyglutarate in IDH-mutated gliomas using two-dimensional localized correlation spectroscopy (2D L-COSY) at 7 Tesla. *J Transl Med*. 2016;14(1):274.

42. Suh CH, Kim HS, Jung SC, Choi CG, Kim SJ. 2-Hydroxyglutarate MR spectroscopy for prediction of isocitrate dehydrogenase mutant glioma: a systemic review and meta-analysis using individual patient data. *Neuro Oncol*. 2018;20(12):1573-1583.

Disclosures

Author Contributions

Conception and design: Nagashima, Iwahashi, Sasayama. Acquisition of data: Nagashima, Iwahashi, Uno, Hashiguchi, Somiya, Komatsu, Hirose, Sasaki. Analysis and interpretation of data: Nagashima, Iwahashi, Uno, Maeyama, Komatsu, Itoh, Sasaki. Drafting the article: Iwahashi. Critically revising the article: Nagashima, Iwahashi, Tanaka, Hirose, Sasaki. Reviewed submitted version of manuscript: Nagashima, Iwahashi, Tanaka, Uno, Hashiguchi. Approved the final version of the manuscript on behalf of all authors: Nagashima. Statistical analysis: Iwahashi, Uno. Administrative/technical/material support: Iwahashi. Study supervision: Tanaka, Sasayama.

Supplemental Information

Correspondence

Hiroaki Nagashima: Kobe University Graduate School of Medicine, Kobe, Hyogo, Japan. hn0628hn@med.kobe-u.ac.jp.